



■ BONE FRACTURE

Development and validation of a modularized external fixator for generating standardized fracture healing micromotions in rats

**W. Qi,
X. Feng,
T. Zhang,
H. Wu,
C. Fang,
F. Leung**

From Li Ka Shing
Faculty of Medicine,
The University of Hong
Kong, Hong Kong,
China

Aims

To fully verify the reliability and reproducibility of an experimental method in generating standardized micromotion for the rat femur fracture model.

Methods

A modularized experimental device has been developed that allows rat models to be used instead of large animal models, with the aim of reducing systematic errors and time and money constraints on grouping. The bench test was used to determine the difference between the measured and set values of the micromotion produced by this device under different simulated loading weights. The displacement of the fixator under different loading conditions was measured by compression tests, which was used to simulate the unexpected micromotion caused by the rat's ambulation. In vivo preliminary experiments with a small sample size were used to test the feasibility and effectiveness of the whole experimental scheme and surgical scheme.

Results

The bench test showed that a weight loading < 500 g did not affect the operation of experimental device. The compression test demonstrated that the stiffness of the device was sufficient to keep the uncontrollable motion between fracture ends, resulting from the rat's daily activities, within 1% strain. In vivo results on 15 rats prove that the device works reliably, without overburdening the experimental animals, and provides standardized micromotion reproductively at the fracture site according to the set parameters.

Conclusion

Our device was able to investigate the effect of micromotion parameters on fracture healing by generating standardized micromotion to small animal models.

Cite this article: *Bone Joint Res* 2021;10(11):714–722.

Keywords: Design for experiments, Surgical instruments, In vivo, Medical treatment, Small animal model, Bone fracture, Bone healing model

Article focus

■ The feasibility and effectiveness of applying standardized micromotion to a rat femur fracture model using a modularized external fixator.

- Systemic error in experimental data caused by the animal's normal activity is negligible.
- The experimental scheme and surgical scheme are safe and effective.
- The experimental results can accurately and quantitatively analyze the fracture healing.

Key messages

- Modularized experimental device reduces the burden on animals.
- Non-contact measurement module based on video identification technology monitors the micromotion parameters in real time.

Strengths and limitations

- Standardized micromotion with various parameters was generated to the rat femur fracture model using an external

Correspondence should be sent to Frankie Leung; email: kkleunga@hku.hk

doi: 10.1302/2046-3758.1011.BJR-2021-0028.R1

Bone Joint Res 2021;10(11):714–722.

fixator of only 12 g by combining the modularized design and the video identification technology.

- The device can produce only axial micromotion but not shear bending and torsion.

Introduction

Micromotion — the cyclical motion of fracture fragments in a small range — is an important biomechanical stimulator of bone-healing.¹ Clinical observations^{2,3} and in vivo animal studies⁴⁻¹² have proved that applied micromotion can accelerate fracture healing, with critical parameters being the range, frequency, duration of motion, and initial timing of motion. However, these parameters of applied micromotion are not yet optimized because previous work has used large animal models, so their corresponding experimental devices are not suitable to optimize parameters of micromotion.

The impact caused by the animal's motion can produce uncontrollable displacement of fracture fragments,^{7,11} which results in considerable systemic error in the experimental data generated from large animal models.^{13,14} Sample size and experimental grouping are also limited by the long experimental time and the great cost of maintaining large animals. Thus, rats with femur fractures are a good animal model for optimizing micromotional parameters, as their advantages include small size, short convalescence, and low feeding cost.^{4,15,16} However, novel fixators and experimental methods do not yet exist to accurately apply the standardized micromotion of various parameters to rat fracture models.

The challenges of using a small animal model in a micromotion study include: 1) difficulties in providing adequate stiffness to such a small fracture site to prevent interference with the experimental results caused by the animal's normal activity;^{17,18} 2) fabricating a lightweight fixator to reduce the interference of the animal's activity;¹¹ and 3) obtaining accurate measurements of the interfragmentary motion.⁹ Weaver et al¹² attempted to investigate the effect of micromotion across a healing fracture on callus properties. Their efforts to separate the heavy adaptor from the main body of the fixator greatly lightened the burden on the experimental animals, and made a rat model in this study possible. However, the "C" type elastic fixator they used does not easily provide axial displacement or enough rigidity to the fracture site. A modularized design for the fixator could be a novel technical route for conducting a bone-healing study.

The aim of this study was to solve the problems of the current experimental devices by: 1) designing an external fixator made of high-strength aluminium alloy with a solid construction; 2) developing a modularized experimental device with dismountable parts to reduce the burden on the experimental animals; and 3) programming a non-contact measurement module based on video identification technology with high measurement accuracy.

We hypothesize that our newly developed modularized fixator can apply standardized micromotion to rat

femur fracture models. The goal is to develop an effective device for investigating the effect of applied micromotion on bone repair. After necessary modifications, the optimal parameters of micromotion in the rat model to promote fracture healing can be used as a valuable reference for surgeons to treat fractures, or for researchers to design fixators.

Methods

Fixator configuration. Our modularized external fixator consisted of the micromotional fixator, an electronic controller, and a non-contact measuring module.¹⁹ The micromotional fixator had a lightweight support, a sliding block, a stepping motor, a threaded rod, a coupling, and four Kirschner wires (K-wires) (Figure 1a). The electronic controller was a commercial single-chip microcomputer based on an A4988 stepping motor driver (Figure 1b).

Non-contact measurement module. The movement of the micromotional fixator was monitored by a non-contact measuring module implemented by a laptop (ThinkPad X1 Carbon Gen 5; Lenovo, China) and a digital camera (GoPro HERO 7 Black; GoPro, USA). The acquired videos were then auto-analyzed to calculate the distance and frequency of the sliding blocking's reciprocating movement using MATLAB (The MathWorks, USA). Figure 1c presents the process of recognizing three red markers (I, II, and III) on the micromotional fixator by the video auto-analysis. The range (R) and the frequency (f) of each micromotion circle in the displacement-time curve were calculated as in Figure 1d. The measuring accuracy of this measuring module was ≤ 0.025 mm in displacement resolution and ≤ 0.04 seconds in time resolution.

Biomechanical assessment. The performance of the micromotional fixator under different loading conditions was validated by setting up a load-simulated facility (Figures 2a and 2b). The hook weights were tied to the sliding block on the fixator through a pulley. In this setup, the fixator bore compressive stress, which mimicked the physiological conditions of fracture healing. The micromotion range (R) and the frequency (f) of the micromotional fixators under different weight-load conditions (0 g to 500 g) were compared. Figure 2c shows the results of the compressive test to predict the uncontrollable micromotion caused by the rat's ambulation. The micromotional fixator was fixed on two artificial bones by four K-wires to simulate the weight status at the fracture site. The two ends of each artificial bone were compressed vertically at 0.5 mm/min from 0 g to 2,500 g using a MTS 858 Mini Bionix (MTS, USA) hydraulic loading machine. The force and displacement data were collected at a sampling rate of 10 Hz. The force-displacement curve was plotted to predict the displacement of the fixator caused by the various daily activities of the rat.

Surgical techniques. In total, 15 female Charles River Sprague-Dawley International Genetic Standardization rats (CD(SD)IGS) (weighing 250 g to 350 g, 12 weeks old) were divided into five groups for different ranges of

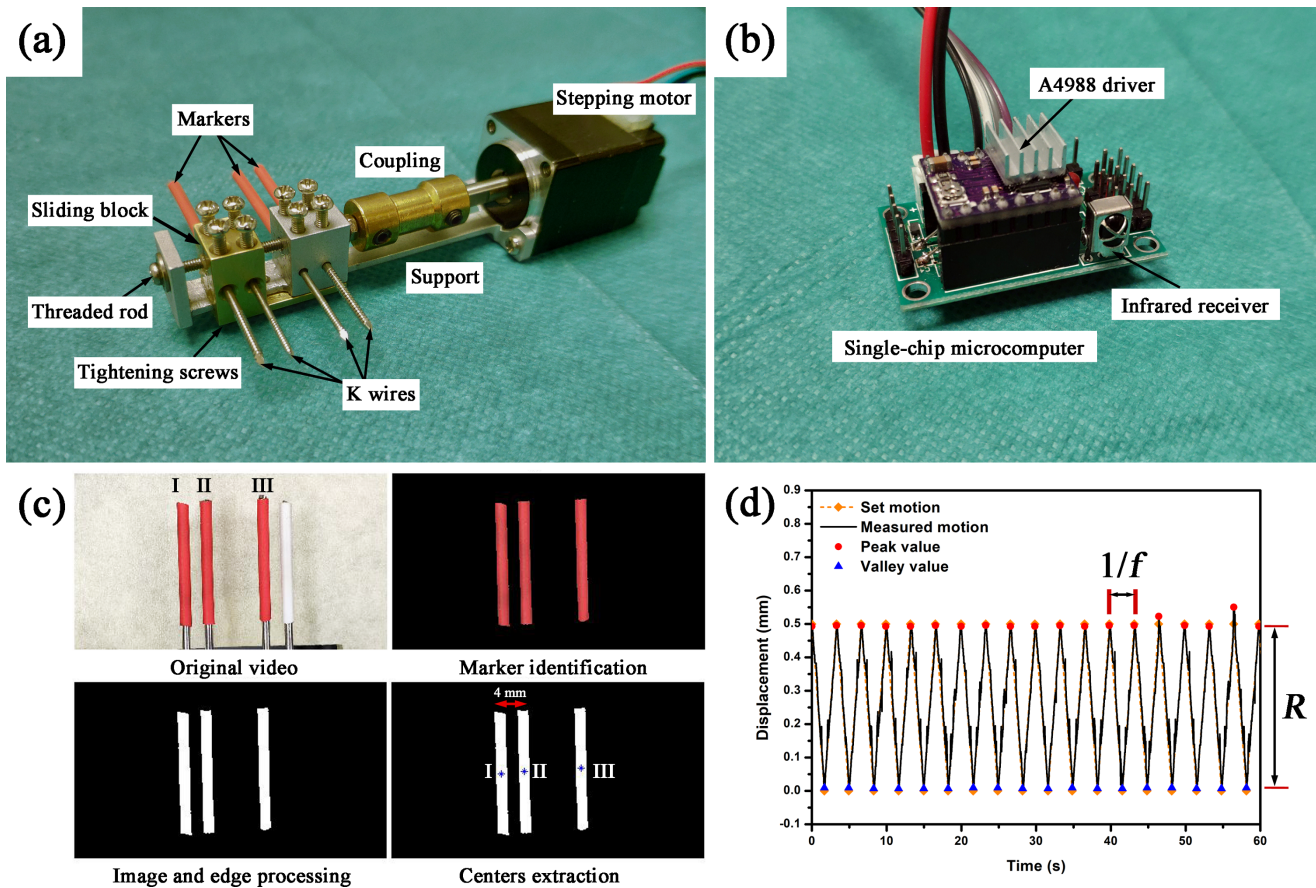


Fig. 1

a) Photograph of the micromotional fixator. b) Photograph of the electronic controller. c) The process of recognizing the three markers (I, II, and III) and calculating the relative displacement of Marker III by video auto-analysis. d) The displacement-time curve of Marker III used to calculate the range (R) and the frequency (f) of each micromotional circle.

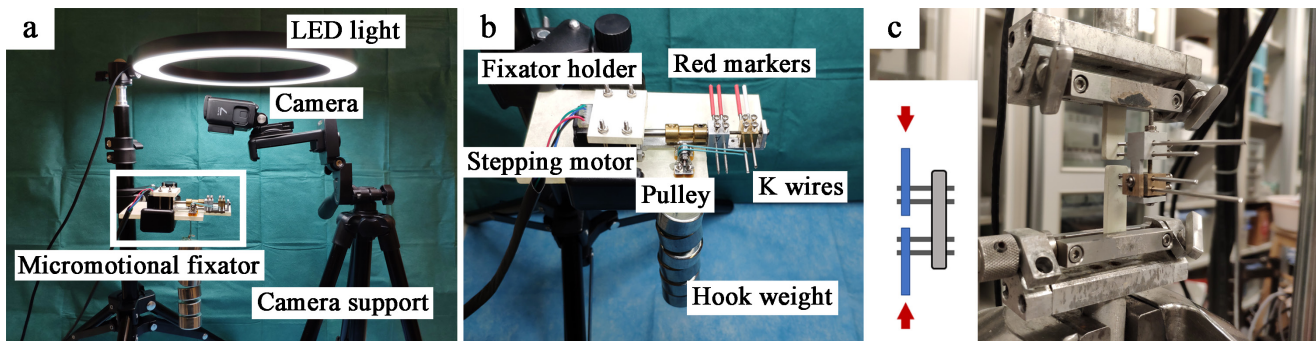


Fig. 2

a) Photograph of the load-simulated facility to validate the effectiveness of the micromotional fixator. b) The enlarged view of the white box indicated in a). c) Photograph of a compressive test to predict the unexpected micromotion caused by the rat's ambulation.

micromotion (0, 0.2, 0.4, 0.6, and 0.8 mm). Rats were anaesthetized with a combination of xylazine (10 mg/kg) and ketamine (100 mg/kg) before conducting the anti-septic surgical procedures. After hair-shaving, for preparation and disinfection, the surgical site was scrubbed with Betadine Scrub (Avrio Health, USA) for at least two minutes, followed by drying with a sterile towel; this scrubbing operation is then repeated for an additional

two minutes and dried with a surgical towel again. For the right femoral shaft defect model, a surgical incision was made to expose bone exposed on the lateral thigh of the rat (Figure 3a) with the periosteum remaining intact. After the femur was exposed, four pilot holes with diameters of 1.2 mm were made from the lateral to medial parts of the femoral shaft using a hand-held electric drill (Meinaite, MNT-998512, China). The drilling

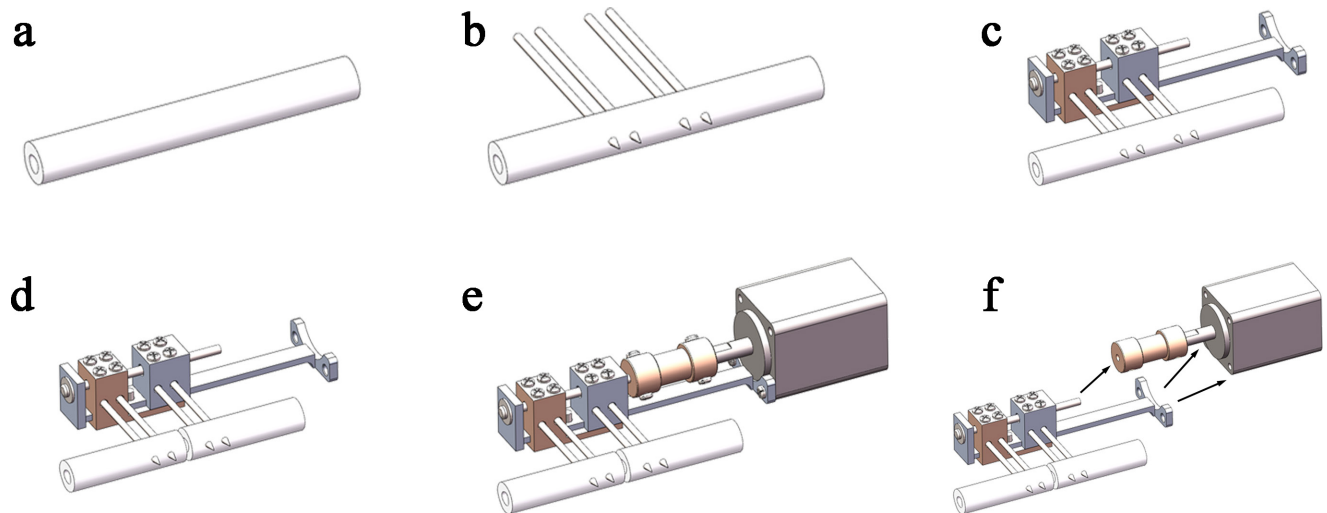


Fig. 3

The schematic diagrams of surgical techniques: a) exposing the femur; b) inserting Kirschner wires after pilot holes were made on the femur; c) installing external fixator; d) making a 2 mm fracture gap before surgical suturing; e) inserting motor after two-week postoperative recovery, then running the stepping motor to apply micromotion to the fracture; and f) dismantling the stepping motor and the coupling after each micromotion application.



Fig. 4

a) Photographs of the surgical incision before suturing showing the external fixator fixed on screwed pins parallel to the femur. b) Photograph of a Sprague Dawley rat carrying the modularized fixator after a two-day postoperative recovery. c) The micromotion was applied after a two-week postoperative recovery; the fixators only worked when the rats were under anaesthesia to decrease potential pain.

positions were determined by a pre-designed guide plate. Subsequently, four screwed pins 1.5 mm in diameter were screwed into the pre-drilled holes (Figure 3b). The external fixator was fixed onto screwed pins to be parallel to the femur (Figure 3c). A 2 mm-long segmental bone defect^{20,21} was then made on the femoral diaphysis between the middle two pins with a wire bone saw (Figure 3d). The periosteum was cut transversely with a 11# scalpel (Swann Morton, UK) to preserve the periosteum at the greatest extent. Figure 4a illustrates the surgical incision and the fracture fixed with the modularized fixator before suturing. Afterwards, the wound was sutured layer by layer, and a proper dressing was applied over the incision. Suturing with a 4/0 Vicryl-coated filament closed the subcutaneous layer, and 3/0 Ethilon was used to close the skin. Terramycin (60 mg/kg) was administered subcutaneously as an antibiotic prophylactic every 72 hours. Buprenorphine (0.05 mg/kg) was subcutaneously injected every 12 hours for three days after surgery as an analgesic.

Standardized micromotion. After surgery, all the animals were allowed normal ambulation with the fixators locked (Figure 4b), except when they were undergoing micromotion application (Figure 3e). The stepping motor and the coupling were removed after each application to ease the weight burden (Figure 3f). After a two-week postoperative recovery, the allocation of experimental groups was determined by rolling a die. The 0 mm group kept rigid fixation and was set as the control group. The experimental groups underwent applied micromotion for two weeks. To decrease the potential pain, the fixators were only activated when the rats were under anaesthesia (Figure 4c). During the application, the measurement module recorded the relative displacement of the fracture ends as videos and calculated the related micromotional parameters, including the micromotional range and micromotional frequency. The cage location is changed weekly, and the other treatment order is determined by the cage location. All the experimental procedures for these animal studies were approved by the Committee

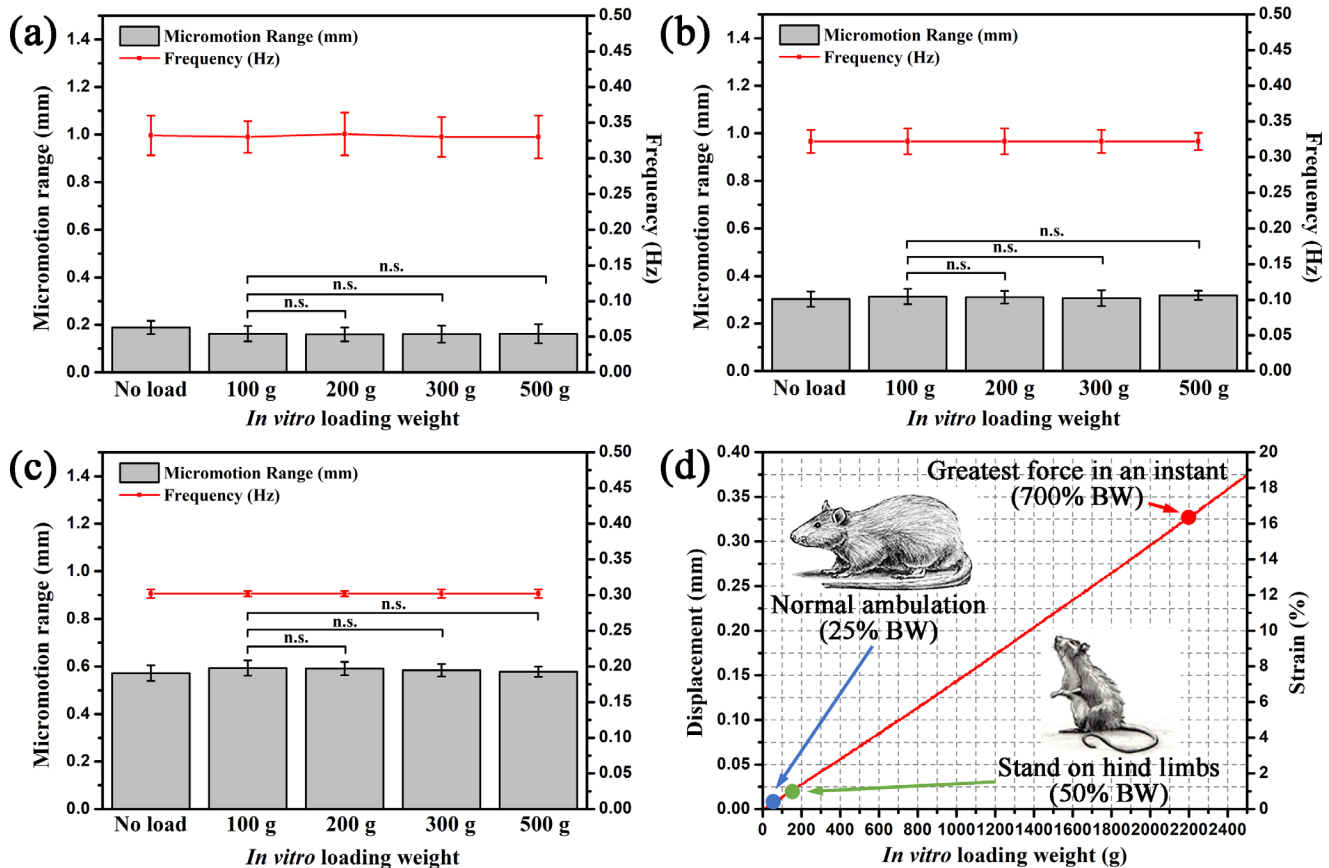


Fig. 5

The simulated load weight (0 g to 500 g) did not affect the range (gray bars) or the frequency (red line) of micromotion in a micromotional range of a) 0.2 mm, b) 0.3 mm, and c) 0.6 mm ($n > 200$ circles, $*p > 0.05$). d) The curve of the loading weight versus displacement/strain of the fixator in the compressive test. The loading conditions during rat's normal ambulation (25% body weight), standing on its hind limbs (50% body weight), and greatest force in an instant (700% body weight) are simulated and represented as coloured dots. BW, body weight; n.s., not significant.

on the Use of Live Animals in Teaching and Research (CULATR No. 4893-18).

Medical imaging assessment. Postoperative radiographs were obtained immediately and then at weekly intervals to quantify the periosteal callus formation. At each time-point, one lateral radiograph was obtained to visualize the anterior, posterior, and lateral cortices without obstruction by the external fixator. All the rats were euthanized at eight weeks after the surgical operation. After the femora were excised, the surrounding soft-tissue, K-wires, and fixator were removed without disturbing the callus around the fracture site. The fractured femora were scanned by micro-CT (SKYSCAN 1076; Bruker, Belgium).

The callus volume (CV) was characterized using CTAn software (Bruker), and the new bone formation evident in the 3D structure was reconstructed with CTVol software (Bruker). A region of interest (ROI) was created encompassing the 2 mm osteotomy site, and any remaining cortical bone was removed from the region. The lateral borders of the ROI were defined by visible mineralization on the outermost boundary of the callus. The gray threshold range used for CT densitometry analysis was 60 to 255 (1,409 to 9,240 in Hounsfield Units). The

resolution was set at 17.34 $\mu\text{m}/\text{pixel}$, and the slice thickness was 17.17 μm .

Statistical analysis. The range and frequency of micromotion was statistically analyzed by a standard two-tailed t -test using Origin software (OriginLab, USA). A value of $p < 0.05$ was considered statistically significant.

Results

Figures 5a to 5c show the consistency of the ranges of R and f of the micromotion stimulation in micromotional ranges of a) 0.2 mm, b) 0.3 mm, and c) 0.6 mm. The number of micromotional cycles was greater than 200 for each group. Each micromotional range showed subtle differences among the no-load group and loading groups in the fit clearance between the sliding block and the driving screw. No statistical significance ($p > 0.05$) was noted between the different weight-load conditions (100 g to 500 g) in all three micromotional ranges. Therefore, a weight loading under 500 g did not affect the reciprocating motion of the sliding block per its pre-set micromotional parameters.

Figure 5d presents the curve of loading weight versus displacement of the fixator in compressive test. The blue

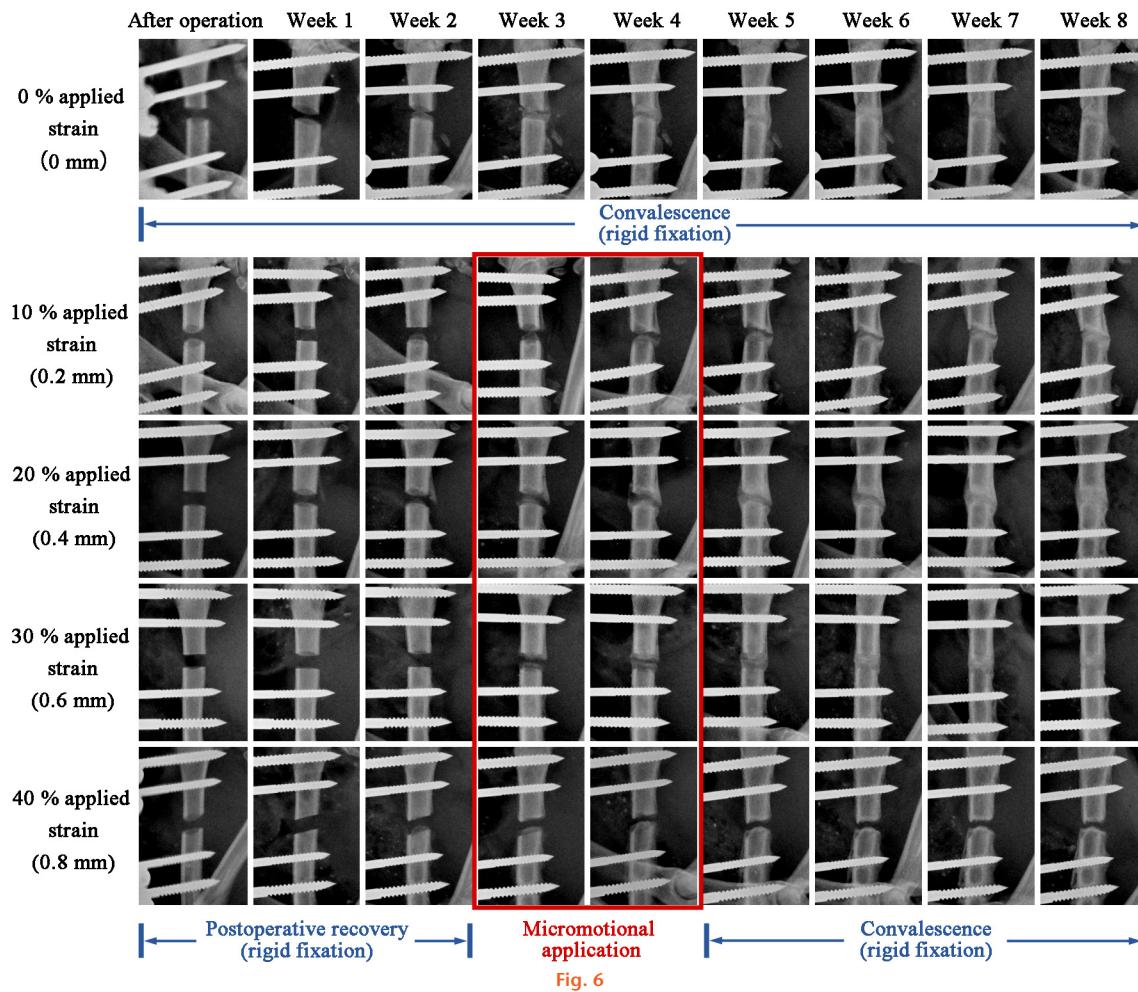


Fig. 6

Postoperative lateral radiographs of the five groups (0 to 40% applied strain) obtained immediately and then at weekly intervals for eight weeks to observe periosteal callus formation. The sizes of the formed calluses were much larger in the 10% and 20% applied strain groups than in the 0% and 30% applied strain groups. A nonunion can be observed in the 40% applied strain group.

dot and the green dot show two loading conditions representing the rat's normal ambulation (25% body weight) and the rat standing on its hind limbs (50% body weight). The axial load of the femur in rats can be up to seven times the body weight,²² which has been indicated by a red dot. The displacement of the fixator has been converted into a strain for a 2 mm fracture gap on the right-hand scale. The compression results demonstrated that the fixator provided enough mechanical stability to the fracture site and that the rat's normal activity brought a small amount (< 1% strain) of unexpected micromotion to the fracture site. Even under the most extreme load, the fixator can limit unexpected micromotion to about 16% strain, indicating a high stiffness of the fixator.

All five groups of rats tolerated the experimental procedure and were able to walk immediately after the operation. All retained a stable fixation of the femoral osteotomy until their euthanization at week 8. Figure 6 presents the postoperative lateral radiographs of one rat in each group (0% to 40% applied strain/0 mm to 0.8 mm), obtained immediately and then at weekly intervals to evaluate

periosteal callus formation. Osteotomy gaps are clearly visible after the operation in all five groups (Figure 6, row 1). At two weeks, small bony periosteal callus formations were visible in all groups (Figure 6, row 3). Micromotion was applied daily from weeks 2 to 4 in the 10% to 40% groups (Figure 6, rows 4 and 5) for 30 minutes per day. The bridging of the periosteal callus was apparent around the fracture ends in all groups, but the unclosed callus gaps in the micromotional groups (10% to 40% applied strain) were more conspicuous than in the non-applied group (0% strain). At the end of week 8 (Figure 6, row 9), the bridging of the periosteal callus was complete around the fracture ends in the 0% to 30% applied strain groups, and the sizes of the formed calluses were much larger in the 10% and 20% applied strain groups than in the 0% and 30% applied strain groups. A nonunion can be observed in the 40% applied strain group.

Micro-CT analysis of the obtained femora suggested that the application of micromotion had a significant impact on repair and that the applied range of micromotion was a critical factor in callus formation.

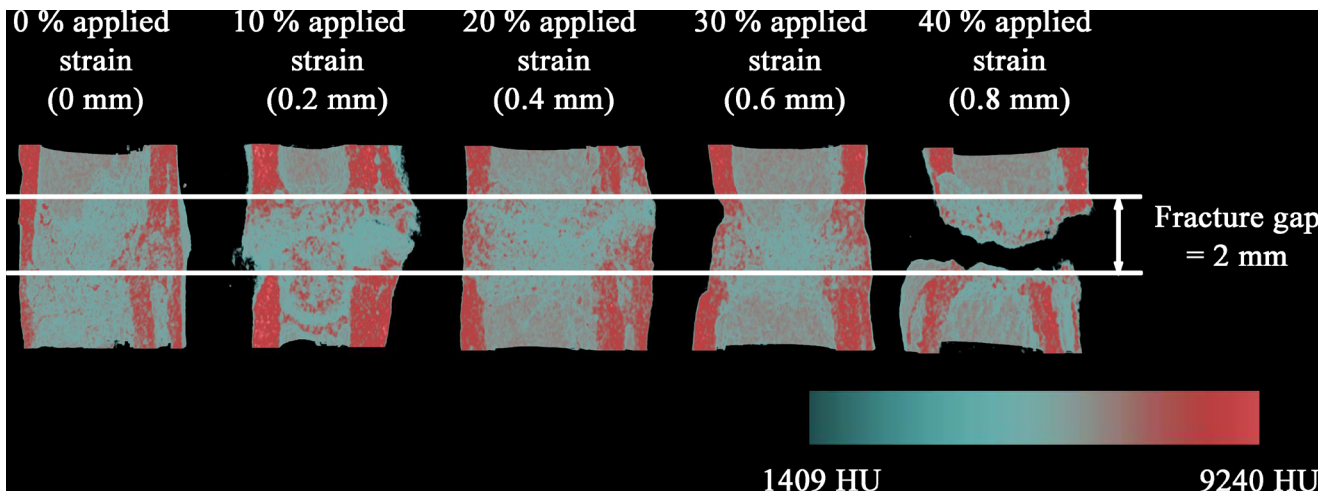


Fig. 7

A comparison of sectional views of the fracture site by micro-CT reconstruction among the five groups (0% to 40% applied strain) after sacrifice at eight weeks after surgery. The callus volumes were significantly greater in the 10% and 20% applied groups than in the 0% and 30% applied groups. A nonunion can be observed in the 40% applied strain group. HU, Hounsfield Unit.

Figure 7 compares sectional views of the fracture sites by micro-CT reconstruction among the five groups (0% to 40% applied strain) after their euthanization at eight weeks post-surgery. The newly generated CV was greater in the 10% strain group than in the other groups. The 10% applied strain group showed about 60% greater mean CV (28.91 mm^3 (SD 3.91)) than the 0% applied strain group (18.12 mm^3 (SD 4.51)), whereas the mean CV of the remaining groups decreased from 22.16 mm^3 (SD 11.0) (20% applied strain group) and 13.85 mm^3 (SD 12.06) (30% applied strain group) to 3.75 mm^3 (SD 6.50) (40% applied strain group) with increasing strain. One rat in the 30% group and two rats in the 40% group experienced nonunion. The CVs of these rats were calculated as zero. Considering the smaller number of samples, no further statistical calculations are given.

Discussion

In this study, the effectiveness of a modularized external fixator was validated under different weight-loading conditions by a load-simulated facility. The uncontrolled micromotion caused by animal activity was estimated by another loading test. The feasibility of using a micromotional fixator and the chosen experimental method were verified with a rat femur fracture model, the preliminary validation of which indicates its reliability and reproducibility in investigations of the effect of applied micromotion on bone healing.

The design of an external fixator for animal experiments to ascertain the effective parameters of applied micromotion to promote fracture healing is a substantial engineering challenge.⁴ The micromotional fixator is supposed to simultaneously meet the following requirements: 1) the fixator should provide sufficient rigidity and stability to the fracture site for healing;^{17,18} 2) the size and weight of the micromotional fixator

should fit the experimental animal's body type to reduce their burden;^{11,17} 3) the electronic controller of the applied micromotion with adjustable parameters;⁹ and 4) the measuring module should monitor the actual displacement of the movable part and make necessary compensation for the error between the measured value and the set value through fine-tuning parameters.¹²

The main body of the micromotional fixator shown in Figure 1a is an electronic linear servo motor actuator, which only allows the sliding block to move along one axis. To reduce the weight of the fixator, aluminium alloy was selected as the material providing the major support of the fixator as it has favourable specific stiffness and specific strength.¹⁸ Considering the demand for abrasive resistance, the sliding block of the fixator was made of brass,²³ and the contact surface was covered with Vaseline lubricant. Once each micromotion application had ended as planned, the stepping motor was dismantled from the coupling to reduce the burden on the experimental animals. The weight of the external fixator (excluding the motor and coupling) was less than 15 g, which had no harmful effects on the daily activity of the rats.^{18,24}

The performance of the micromotional fixator was verified by establishing a load-simulated facility (Figures 2a and 2b) to mimic the stress state of the fixator on experimental animals by tying hook weights of varying weights onto the sliding block. The verification results (Figures 5a to 5c) showed that the effect of weight-loading was negligible on the operation of the micromotional fixator. In addition, as a determined value for each fixator, the fit clearance between the sliding block and driving screw was eliminated by the parameter settings in our further experiments.

The random, unexpected motion caused by animal ambulation or other daily activity is a common system error that was predicted by a compressive test.¹⁸ In the compressive test, the effect of two usual postures — standing still on four feet and standing on the hind limbs — has been of particular concern. The mechanical test results showed that the fixator had enough rigidity to protect the fracture site from the interference of unexpected motion. This study omitted the bending test and the torsion test because the compressive test is a standard method of evaluating stiffness for the design and characterization of external fixators.²⁵ The specially designed structure furnished our experimental fixator with more stability on bending and torsion than on compression.

In our *in vivo* animal test, all the rats with femoral defects fixed by our specially designed external fixator could walk normally after surgery and after micromotion application. This indicated that the installation of our external fixator and the micromotion it provided were feasible and safe for the rats. The radiographs and micro-CT results (Figures 6 and 7) showed that the volumes and morphologies of calluses were determined by the applied range of micromotion. Our limited animal samples showed that when the applied micromotion was at 10% and 20% strain levels, the fracture healing was improved, compared to the non-application group. In contrast, an applied micromotion that exceeded 30% strain resulted in delayed union and nonunion. Some previous studies on large animal models, like sheep and rabbits,¹ speculated that an effective micromotional range exists for bone healing acceleration, which is consistent with our preliminary *in vivo* data. However, the specific strain range remains unclear and requires further investigation.⁴ Our *in vitro* and *in vivo* results confirmed that the modularized external fixator can provide enough stability to a fracture site, and with little interference to the experimental animal, to generate accurate micromotion to the fracture gap. Therefore, our device has strong potential for use in small animals to further explore the optimal strain to accelerate fracture healing.

This study has one notable limitation: we simplified the experiment by only allowing the compression test to estimate the micromotion linearly. This study did not consider the bending and torsion caused by the rat's activities, so unexpected micromotion at the fracture site could mean that the value is higher than 1% strain when the rat is involved in intensive activities. Further animal tests are needed to further quantify the influence of motions in other directions. Another limitation of the study was the small number of animals used. However, the experimental results obtained from 15 rats show that the experimental method and device are effective and that micromotional parameters can affect fracture healing. The effect of micromotional parameters on fracture healing must be investigated in a follow-up experiment with a larger sample size.

Supplementary material



ARRIVE checklist.

References

1. Elliott DS, Newman KJH, Forward DP, et al. A unified theory of bone healing and nonunion. *Bone Joint J.* 2016;98-B(7):884–891.
2. Kenwright J, Richardson JB, Cunningham JL, et al. Axial movement and tibial fractures. A controlled randomised trial of treatment. *J Bone Joint Surg Br.* 1991;73-B(4):654–659.
3. Stewart S, Darwood A, Masouros S, Higgins C, Ramasamy A. Mechanotransduction in osteogenesis. *Bone Joint Res.* 2020;9(1):1–14.
4. Jagodzinski M, Krettek C. Effect of mechanical stability on fracture healing—an update. *Injury.* 2007;38 Suppl 1:S3–10.
5. Bishop NE, van Rhijn M, Tami I, Corveleijn R, Schneider E, Ito K, et al. Shear does not necessarily inhibit bone healing. *Clin Orthop Relat Res.* 2006;443:307–314.
6. Augat P, Merk J, Wolf S, Claes L. Mechanical stimulation by external application of cyclic tensile strains does not effectively enhance bone healing. *J Orthop Trauma.* 2001;15(1):54–60.
7. Claes L, Eckert-Hübner K, Augat P. The effect of mechanical stability on local vascularization and tissue differentiation in callus healing. *J Orthop Res.* 2002;20(5):1099–1105.
8. Yamaji T, Ando K, Wolf S, Augat P, Claes L. The effect of micromovement on callus formation. *J Orthop Sci.* 2001;6(6):571–575.
9. Hente R, Füchtmeier B, Schlegel U, Ernstberger A, Perren SM. The influence of cyclic compression and distraction on the healing of experimental tibial fractures. *J Orthop Res.* 2004;22(4):709–715.
10. Goodship AE, Cunningham JL, Kenwright J. Strain rate and timing of stimulation in mechanical modulation of fracture healing. *Clin Orthop Relat Res.* 1998;355:S105.
11. Matsushita T, Kurokawa T. Comparison of cyclic compression, cyclic distraction and rigid fixation. Bone healing in rabbits. *Acta Orthop Scand.* 1998;69(1):95–98.
12. Weaver AS, Su Y-P, Begun DL, Miller JD, Alford AI, Goldstein SA. The effects of axial displacement on fracture callus morphology and MSC homing depend on the timing of application. *Bone.* 2010;47(1):41–48.
13. Schmidt-Bleek K, Petersen A, Dienelt A, Schwarz C, Duda GN. Initiation and early control of tissue regeneration - bone healing as a model system for tissue regeneration. *Expert Opin Biol Ther.* 2014;14(2):247–259.
14. Park SH, O'Connor K, McKellop H, Sarmiento A. The influence of active shear or compressive motion on fracture-healing. *J Bone Jt Surg Am.* 1998;80-A(6):868–878.
15. Hjorthaug GA, Søreide E, Nordsletten L, et al. Short-term perioperative parecoxib is not detrimental to shaft fracture healing in a rat model. *Bone Joint Res.* 2019;8(10):472–480.
16. Wang C, Zheng G. F, Xu X. F. Microrna-186 improves fracture healing through activating the bone morphogenetic protein signalling pathway by inhibiting smad6 in a mouse model of femoral fracture: An animal study. *Bone Joint Res.* 2019;8(11):550–562.
17. Epari DR, Schell H, Duda GN, Kassi J-P. Timely fracture-healing requires optimization of axial fixation stability. *J Bone Jt Surg Am.* 2007;89-A(7):1575–1585.
18. Willie B, Adkins K, Zheng X, Simon U, Claes L. Mechanical characterization of external fixator stiffness for a rat femoral fracture model. *J Orthop Res.* 2009;27(5):687–693.
19. Qi W, Feng X, Zhang T, Frankie Ka-Li L. The development and *in vivo* validation of an external fixation device with standardized micromotion for accelerating fracture healing. *Annu Int Conf IEEE Eng Med Biol Soc.* 2020;2020:5167–5170.
20. Claes LE, Heigele CA, Neidlinger-Wilke C, et al. Effects of mechanical factors on the fracture healing process. *Clin Orthop Relat Res.* 1998;355:S132.
21. Meeson R, Moazen M, Sanghani-Kerai A, Osagie-Clouard L, Coathup M, Blunn G. The influence of gap size on the development of fracture union with a micro external fixator. *J Mech Behav Biomed Mater.* 2019;99:161–168.
22. Wehner T, Wolfram U, Henzler T, Niemeyer F, Claes L, Simon U, et al. Internal forces and moments in the femur of the rat during gait. *J Biomech.* 2010;43(13):2473–2479.
23. Mark H, Bergholm J, Nilsson A, Rydevik B, Strömberg L. An external fixation method and device to study fracture healing in rats. *Acta Orthop Scand.* 2003;74(4):476–482.
24. Namkung-Matthai H, Appleyard R, Jansen J, et al. Osteoporosis influences the early period of fracture healing in a rat osteoporotic model. *Bone.* 2001;28(1):80–86.

25. **Glatt V, Evans CH, Matthys R.** Design, characterisation and in vivo testing of a new, adjustable stiffness, external fixator for the rat femur. *Eur Cell Mater.* 2012;23:289–298.

Author information:

- W. Qi, PhD, Postdoctoral Fellow
- T. Zhang, MD, Research Assistant Professor
- H. Wu, BS, MPhil Student
Department of Orthopaedics and Traumatology, Li Ka Shing Faculty of Medicine, The University of Hong Kong, Hong Kong, China.
- X. Feng, MD, PhD, Postdoctoral Fellow, Orthopaedic Surgeon, Department of Orthopaedics and Traumatology, Li Ka Shing Faculty of Medicine, The University of Hong Kong, Hong Kong, China; Yangjiang People's Hospital, Yangjiang, China.
- C. Fang, MBBS, Deputy Chief of the Division of Orthopaedic Trauma
- F. Leung, MBBS, Division Chief, Division of Orthopaedic Trauma
Department of Orthopaedics and Traumatology, Queen Mary Hospital, The University of Hong Kong, Hong Kong, China.

Author contributions:

- W. Qi: Writing – original draft, Methodology.
- X. Feng: Writing – review & editing, Validation.
- T. Zhang: Formal analysis.
- H. Wu: Data curation.
- C. Fang: Project administration.

- F. Leung: Supervision.
- W. Qi and X. Feng contributed equally to this work.

Funding statement:

- This study was funded by a research grant from AO Trauma Asia Pacific (Project number AOTAP19-13). No benefits in any form have been received or will be received from a commercial party related directly or indirectly to the subject of this article.

Acknowledgements:

- We wish to give special thanks to our technicians in the Department of Orthopedics and Traumatology, the University of Hong Kong (HKU) for their assistance and support of this project: Mr. Stephen Chan, Mr. Tony Liu, Ms. Kammy Yip, and Ms. Helen Chan. We would also like to express our appreciation to all staffs in the Laboratory Animal Unit, the Centre for Comparative Medicine Research (CCMR), HKU Faculty of Medicine.

Open access funding

- The authors confirm that the open access funding for this study was covered by the research grant from AO Trauma Asia Pacific (Project number AOTAP19-13).

© 2021 Author(s) et al. This is an open-access article distributed under the terms of the Creative Commons Attribution Non-Commercial No Derivatives (CC BY-NC-ND 4.0) licence, which permits the copying and redistribution of the work only, and provided the original author and source are credited. See <https://creativecommons.org/licenses/by-nc-nd/4.0/>